applied sciences

MDPI

Article

Preliminary design of a self-sufficient electrical storage system based on electrolytic hydrogen for power supply in a residential application

C. G. Sacedón[1], E. López-Fernández[1], A.R. de la Osa[1], F. Dorado[1], E. Amores[2], A. de Lucas-Consuegra[1*]

[1] Department of Chemical Engineering, Faculty of Chemical Sciences and Technologies, University of Castilla-La Mancha, Avda. Camilo José Cela 12, E-13071, Ciudad Real, Spain.

[2] Centro Nacional del Hidrógeno (CNH2). Prolongación Fernando El Sant o s/n, 13500 Puertollano, Ciudad Real, Spain.

* Corresponding author: Antonio.LConsuegra@uclm.es

Citation: Gómez Sacedón, C; de Lucas-Consuegra, A. Preliminary design of a self-sufficient electrical storage system based on electrolytic hydrogen for power supply in a residential application. *Energies* **2021**, *14*, x. https://doi.org/10.3390/xxxxx

Academic Editor: Firstname Lastname

Received: date

Accepted: date

Published: date

Publisher's Note: MDPI stays neutral with regard to jurisdictional claims in published maps and institutional affiliations.

Abstract: The use of renewable energy and hydrogen technology is a sustainable way to be the solution for the intermittent feature of renewable energies. Hence, the aim of the present work is to design a self-sufficient system for a one-family house by coupling a solar photovoltaic array and an anion exchange membrane water electrolyzer (AEMWE). The first step is the selection of the photovoltaic panel by using a software PV-SYST 7.0. Then, the hydrogen production system is calculated by coupling the electrolyzer and photovoltaic panel current-potential curves. A fuel cell is selected to use the hydrogen produced when the solar energy is not available. Finally, the hydrogen storage tank is also estimated to store hydrogen for a design basis of four consecutive cloudy days according to the hydrogen consumption of the fuel cell. The whole system is designed by a simple procedure for a specific location in Ciudad Real (Spain) for January, known as the coldest month of the year. The simple procedure described in this work could be used elsewhere and demonstrated that the hydrogen production at low scale is a suitable technology to use renewable energy for self-energy supporting in a residential application without any connection to the grid.

Keywords: Photovoltaic Coupling; Alkaline Exchange Membrane Water Electrolyzer; Hydrogen; Renewable Energy; Electrical energy storage.

1. Introduction

Renewable energy sources are the solution for the negative environmental impact of fossil fuel combustion and the dependence on oil producing countries. However, the dependence of renewable energy on weather conditions makes it to be intermittent [1,2]. Hydrogen is an energy vector that can be coupled to renewable energy sources with many applications in residential, transportation and industries as an energy storage. However, the efficient production and the storage persist as a problem which is necessary to solve [3].

Water electrolysis is a way to obtain pure hydrogen in combination with renewable energy such as photovoltaic or wind energy. Anion exchange membrane water electrolyzers (AEMWE) is a technology that starts to be available in the electrolyzer market. Recently, AEMWE has attracted much attention due to its advantages in comparison to other traditional electrolyzers, e.g. alkaline water electrolyzers (AWE), solid oxide electrolyzer cell (SOEC) and proton exchange membrane water electrolyzers (PEMWE) [4–6]. AEMWE combines the advantage of conventional alkaline electrolysis (in terms of cost) and PEM (in terms of production capacity and purity of hydrogen), so it can become the key electrolysis technology for the future. These new designs aim at reducing ohmic overpotentials. In this way, higher current densities are achieved, thus, improving electrolysis efficiency [7].

On the other hand, photovoltaic (PV) energy is an excellent and clean renewable energy source [8]. Any photovoltaic unit depends on the solar irradiation and temperature. However, due to this variation the solar energy needs to be coupled with an energy storage unit. Nowadays, this coupling is typically performed by using a battery [9], which stores renewable energy in form of chemical energy but with important limitations in terms of capacity and lifetime. It is useful when the solar energy is not enough for covering the electrical demand of a house since an amount of energy is kept in the battery [10].

One interesting alternative to these conventional systems could be the use of the electrolysis-fuel cell technology so called "hybrid alternative energy system" [11], which uses the excess of energy produced in a water electrolyzer to generate hydrogen. Later, hydrogen, which can be easily stored, is transformed into electricity by using a fuel cell when photovoltaic renewable energy is not available [12–15]. In order to get a maximum global efficiency, the coupling between the photovoltaic panel and the electrolyzer must be performed at the maximum power point (MPP) of the photovoltaic system [16,17]. Different strategies can be found in the available literature for the design of combined PV, electrolyzer and fuel cell systems. A combination of empirical electrochemical relationships, thermodynamics, and heat transfer theory is used in many reports of a hybrid wind-PV system performance investigation [2][9]. Other reports use energy-exergy and economic analyses of the hybrid solar-hydrogen renewable energy system [12,13]. The optimization of the photovoltaic-hydrogen supply system of a stand-alone by a remote-telecom application has also been studied [14]. A comprehensive methodology to size, analyse and assess PV-H_2 systems concerns to many researchers that have reported different works on the energy balance and the efficacy of the system in terms of the levels of energy stored and the loading requirements [18,19].

The current manuscript examines the direct coupling between a PV panel and an AEMWE using the tools available in the market, for instance, the use of the commercial PV-SYST software. Nowadays, the proposed coupling (PV panel and AEMWE) is a novelty since it is mostly carried out with PEMWE or AWE. The stack lifetime, the degradation and the energy consumption are some advantages of AEMWE. The idea is to design a self-sufficient system for a residential application, i.e. for one-family house by a general and simple procedure that could be used elsewhere for other similar applications. The whole system is calculated and designed for a specific location in Ciudad Real (Spain) in January, the coldest month of the year with the lowest radiation level.

2. Methodology

2.1 General design considerations

The first design basis considers the typical electrical energy charges for a one-family house as shown in Fig. 1, where energy and hour daily operation are included for a day [17]. As can be observed from the figure, the peak hour is at 8 p.m. when the total electrical energy requirement increases up to 1015 Wh, being the period with the higher electrical energy consumption from 8 p.m. to 11 p.m. This is a daily typical profile of electrical energy charges for a Spanish house, which may widely vary depending on the country. Hence, the total amount of electrical demand per day for this case of study is 7.635 kWh/day.

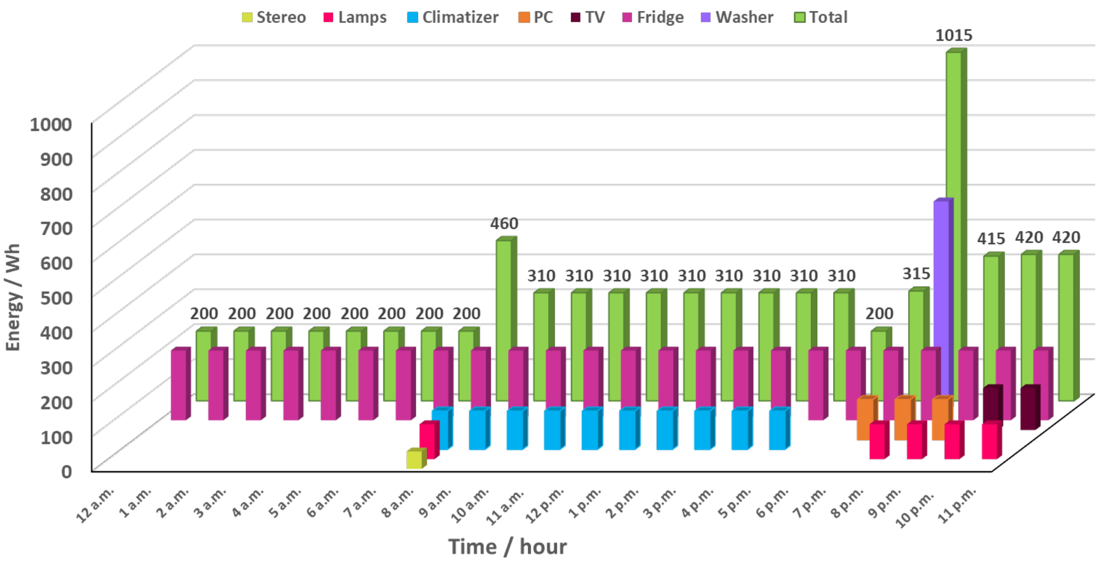

Figure 1. Electrical demand of a one-family house [17].

The second design consideration is the temporal horizon of the full month of January. Considering that this month is characterized by the lowest radiation level, and it is known to be the coldest one, if the electrical demand is supplied by the proposed, designed system, it could be generally considered that those requirements for any other month will be fulfilled too. Hence, our specific case of study considers weather data of Ciudad Real, a city located in Spain. As design basis, the electrical demand is the same for all days.

The third design basis considers that the amount of energy to be stored in form of hydrogen should be enough for self-supplying the house for four consecutive days without any PV energy production since it is based on the meteorological data from this city supplied by the PV-SYST software and january is the most restrictive month with four consecutive days without any radiation at all. Thus, if there is a cloudy day or not enough solar radiation is available, the house can receive the stored energy in form of hydrogen via a fuel cell. The electrical demand of the house for four days is 30.54 kWh. Hence considering the hydrogen consumption of the fuel cell for supplying this electrical demand, the amount of hydrogen to consider is 1.8 kg which is the design basis for the hydrogen storage tank. Another base design is the efficiency of both the fuel cell and electrolyzer, i.e., 73.5% and 45%, respectively.

2.2 Design path

The design path is shown in Fig. 2. Firstly, the PV module is selected with PV-SYST 7.0, a powerful and commercially available software for designing photovoltaic systems [20]. The electrical energy charges (previously analysed), geographic location and period of time (month) are the input variables to the software for the PV calculation [21]. Furthermore, a universal regulator is into the system. Note that although a battery is required by the software in order to perform the calculations, it will be lately replaced by the electrolyser-fuel cell system for the electrical energy storage. Hence, the aim of this first step is to calculate a preliminary solar PV array for self-electrical energy consumption and battery storage by direct coupling without any converter and MPP tracker as coupling system [22–25]. However, in other configurations it is possible to include a battery with the electrolyzer to store rapid power fluctuations or in those situations where the AEM electrolyzer is not worth turning it on.

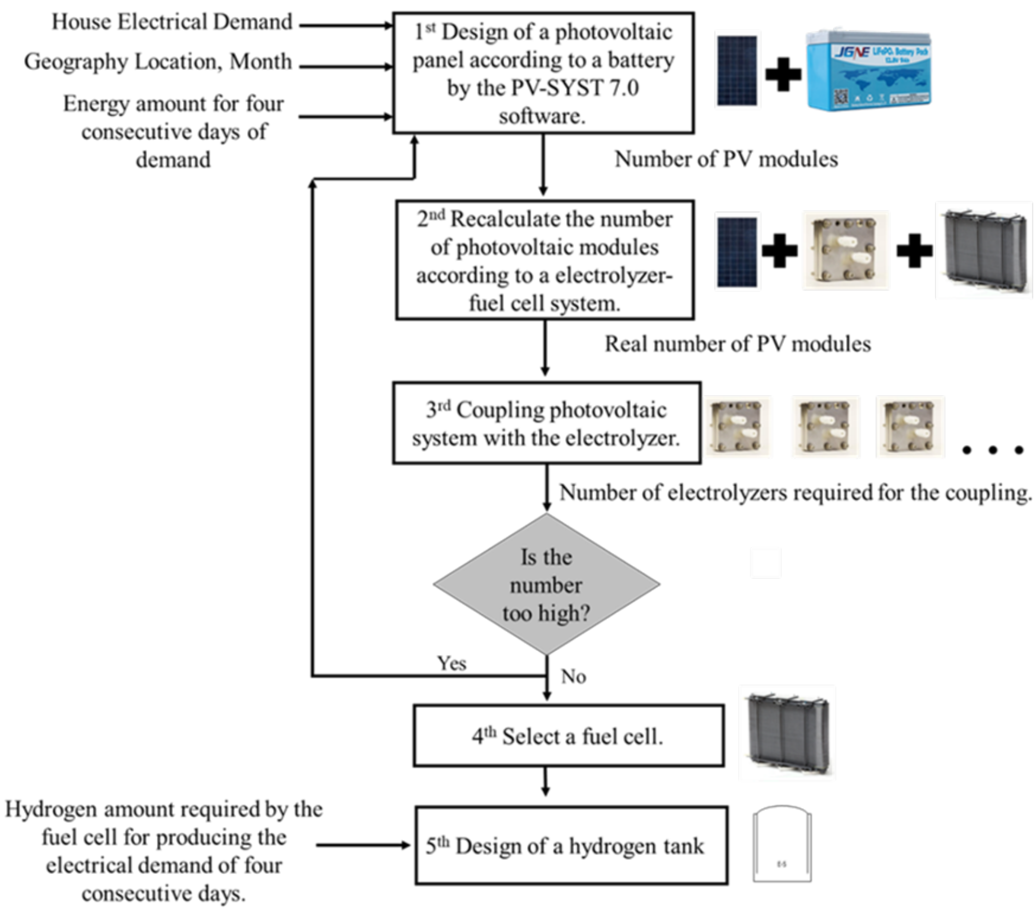

Figure 2. Flow-chart of design.

In the second step, the preliminary number of PV modules estimated by the software will be recalculated by replacing the battery by the experimental electrolyzer curve obtained in our lab (that will be described below) and a commercial fuel cell [26]. Considering that the overall efficiency of the electrolyzer-fuel cell used for energy storage is much lower than that of the battery (90-95 %) [27], the final number of PV modules would be recalculated according to an energy balance. Once the PV_P is designed, the coupling of PV-EL is the next step. It is based on the coupling of the current-potential curves of the experimental electrolyzer cell and the PV module at the maximum power point of the latter. By this way, the final number and area of the electrolysis cells can be obtained. It is a practical strategy that can be used by the electrolyzer manufactures.

Then, the fuel cell is selected according to the highest hourly energy consumption value of the house (1015 Wh). Finally, the hydrogen storage tank is designed considering that hydrogen should be stored for four consecutive days without any further production. The complete system is shown in the Fig. S1 in the supporting information.

3. Results and discussions

In this section the most relevant results and calculations will be shown for the four main components of the whole system: the solar PV array, the electrolyzer, the hydrogen tank and the fuel cell.

3.1. Photovoltaic panel

The preliminary design of the solar PV array is based on PV-SYST 7.0, one useful software for the design of photovoltaic system anywhere in the market [20]. It allows to define an independent system or a general electric grid. In this work the system is independent since it is a one-family house, which must be electrically isolated. The electrical charge (shown in the Fig. 1) was introduced in the software for the initial calculation of the number of PV modules and the energy storage system in chemical form with a battery.

The type of PV module is chosen from a list provided by the software, considering the maximum current of the module and the electrolyzer [26]. Hence, taking into account that the maximum current point of the electrolyzer is 4 A, according to the experimental polarization curve obtained in our group, the selected PV is the model *Solartec SST72 110 24 106W module* with a maximum current of 3.3 A. Agree with this, the PV module to choose would have a maximum current point (I_{MPP}) lower than 4 A. This PV selected module is based on mono-crystalline silicon (c-Si), which is the most common ones with standard dimensions of 1303x666 mm [24,25]. The I-V characteristic curves for the selected module at different solar radiation levels is also displayed by the software as shown in Fig. S2 of the supporting information.

On the other hand, the battery system should also be considered at this time. According to the design basis of 4 consecutive days without any PV production and the electrical energy charges of our case of study, a battery with a power capacity higher than 30.54 kWh must be selected. In this case, from the list provided by the software the selected battery is one with 32.3 kWh of power capacity. The model is *Cell HTCFR26650-3800mAh-3.2V*. The capacity is 749 Ah and the voltage 48 V. Note that the software warns if the battery is appropriate or not for the application.

Once the specific types of PV module and battery are chosen, the number of PV modules displayed in series in the solar PV array is introduced in the PV-SYST 7.0 software following an optimization procedure, as described below. In this case the aim is to find the minimum number of PV modules which allows to provide enough electrical energy for all the days of January to avoid that the energy run out with the combined Photovoltaic-Battery system. This optimization procedure is performed according to the curves displayed by the software, which shows the electrical power demand covered by the system and the loss of energy associated with the fully charged battery (Fig. 3). In this case, special attention should be paid to find the lowest number of PV modules which avoids the loss of power demand (green line, secondary axis of Fig. 3) for different temporal horizons. This optimization has started with sixteen PV modules in series (Fig. 3a). In this case, it can be observed that for the temporal horizon of one day (1st January) the system can self-supply the house and the battery is not full since a loss of energy is not shown in the graph. On the other hand, as can be observed from Fig. 3b, keeping this number of PV modules, the electrical energy demand of the house for a whole week is not covered (the first week of January). Hence, at the seventh day, the house does not receive any electricity since the battery has not received enough energy to be used later. Therefore, the number of PV modules should be increased to completely charge the battery for its further use. In this sense, the optimization continues with twenty-two PV modules. In this case (as can be observed on Fig. 3c), the electrical demand is fully covered for self- supporting the house for the first week, but it seems not to be enough for the second one since the power demands fall to zero after the ninth day (as shown in the Fig. 3d). The procedure is then repeated for twenty-eight (Fig. 3e) and thirty PV modules (Fig. 3f), being this latter, the minimum number of PV modules required for covering the whole month of January. According to this analysis, thirty PV modules and a battery with 32.3 kWh of power capacity fulfil the preliminary design of the energy-production and storage system.

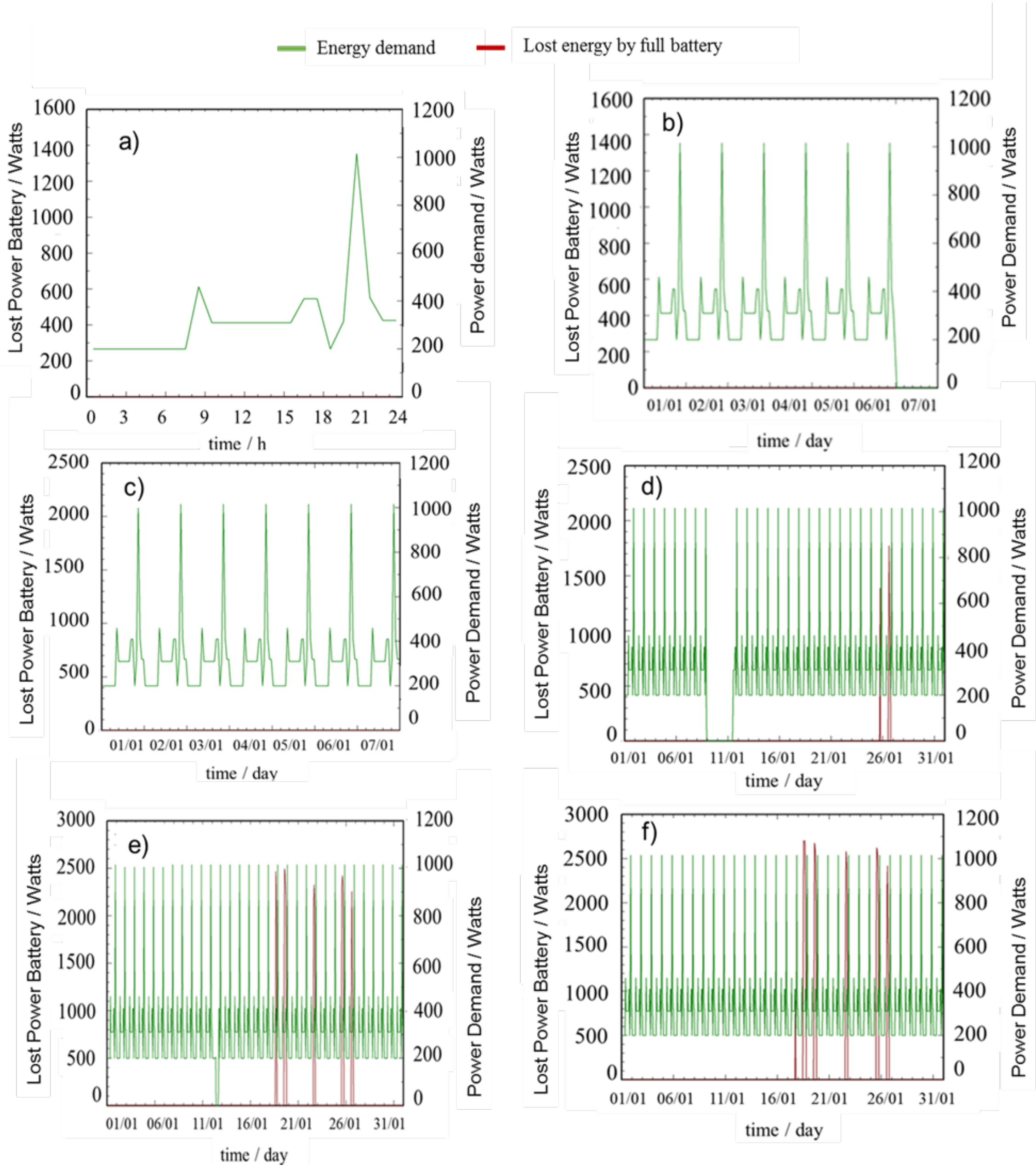

Figure 3. January supplied electrical demand by a) sixteen PV modules for the 1st day b) sixteen PV modules for the first week c) twenty-two PV modules for the first week d) twenty-two PV modules for the full month e) twenty-eight PV modules for the full month f) thirty PV modules for the full month.

The next step deals with the recalculation of the number of PV modules according to our new proposed energy storage system, which replaces the battery by an EL-FC. At this point it should be noted that the software provides the output energy of the photovoltaic system ($E_{o,PV30m}$), which has thirty PV modules, the optimal number for supplying the electrical demand. Part of this energy is directly used by the one-family house (D) and the excess energy ($E_{e,PV30m}$) is introduced to the battery. Both provided values of energy are shown in Table 1, along with the electrical demand per day. With the efficiency of the battery (90%), its output energy ($E_{o,BA}$) is calculated, also shown in Table 1. This value should be equal to the output energy of the fuel cell ($E_{o,EL\text{-}FC}$) considering the efficiency of the electrolyzer and fuel cell [28–33].For that purpose an energy balance is now performed (as shown in Fig. 4) to finally calculate the value of the input energy of the electrolyzer ($E_{i,EL}$). Furthermore, there is an important consideration about the state of charge of the battery since the software considers that the battery has previous year´s surpluses. However, it can continue to charge because it is not totally full.

Table 1. Photovoltaic panel energy, battery energy and electrolyzer energy.

t (days)	$E_{o,PV30m}$ (kWh/day)	$E_{e,PV30m}$ (kWh/day)	$E_{o,BA}$ (kWh/day)	$E_{i,EL}$ (kWh/day)	$E_{i,BAe}$ (kWh/day)	$E_{e,PVn}$ (kWh/day)
1	14	6.365	5.729	17.314	1.731	19.045
2	6.81	0.000	0.000	0.000	0.000	0.000
3	4.613	0.000	0.000	0.000	0.000	0.000
4	7.021	0.000	0.000	0.000	0.000	0.000
5	13.65	6.015	5.414	16.362	1.636	17.998
6	6.598	0.000	0.000	0.000	0.000	0.000
7	1.697	0.000	0.000	0.000	0.000	0.000
8	5.79	0.000	0.000	0.000	0.000	0.000
9	7.528	0.000	0.000	0.000	0.000	0.000
10	4.938	0.000	0.000	0.000	0.000	0.000
11	4.883	0.000	0.000	0.000	0.000	0.000
12	15.78	8.145	7.331	22.155	2.216	24.371
13	16.51	8.875	7.988	24.141	2.414	26.555
14	4.798	0.000	0.000	0.000	0.000	0.000
15	10.5	2.865	2.579	7.793	0.779	8.572
16	10.14	2.505	2.255	6.814	0.681	7.495
17	18.53	10.895	9.806	29.636	2.964	32.599
18	6.235	0.000	0.000	0.000	0.000	0.000
19	8.691	1.056	0.950	2.872	0.287	3.160
20	3.597	0.000	0.000	0.000	0.000	0.000
21	11.45	3.815	3.434	10.377	1.038	11.415
22	10.07	2.435	2.192	6.623	0.662	7.286
23	5.58	0.000	0.000	0.000	0.000	0.000
24	11.45	3.815	3.434	10.377	1.038	11.415
25	7.557	0.000	0.000	0.000	0.000	0.000
26	8.529	0.894	0.805	2.432	0.243	2.675
27	1.435	0.000	0.000	0.000	0.000	0.000
28	1.357	0.000	0.000	0.000	0.000	0.000
29	1.593	0.000	0.000	0.000	0.000	0.000
30	17.85	10.215	9.194	27.786	2.779	30.565
31	20.24	12.605	11.345	34.287	3.429	37.716

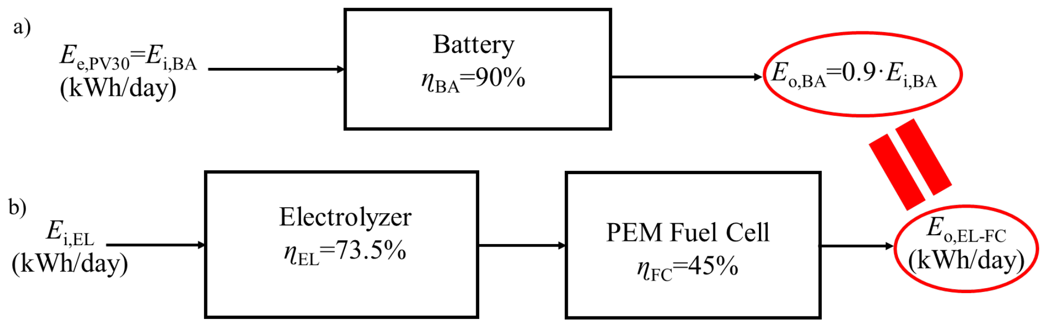

Figure 4. The energy balance of two systems a) battery system b) electrolyzer-fuel cell system.

The calculation of $E_{i,EL}$ value for each specific day is performed by using Eq. (1), obtained from the energy balance schematically shown in Fig. 4b, which requires the efficiency of the electrolyzer (η_{EL}) and fuel cell (η_{FC}).

$$E_{O,EL-FC} = \eta_{EL} \cdot \eta_{FC} \cdot E_{i,EL} \quad (1)$$

The obtained values are summarized in Table 1, along with the values of the following reported parameters: energy of the back-up battery ($E_{i,Bae}$) and excess of solar energy ($E_{e,PVn}$). At this point it should be noted that an oversizing is performed in order to keep 10 % of energy as a backup battery ($E_{i,BAe}$) since most of the strategies found in literature use a battery as an additional storage notwithstanding the hydrogen tank [34–38].

Taking into account the extra energy that the solar PV array must produce using the EL-FC instead of the battery, an oversizing factor can be calculated by Eq. (2) considering the relation between the solar PV array energy of the proposed system and that of the preliminary solar PV array of thirty PV modules. The obtained sizing factor is 3, which means that the final number of PV modules required with our new storage system is ninety. The proposed system requires more PV modules because of the efficiency of a battery (90%) is higher than the efficiency of the EL-FC system (33%) as known. However, the charge/discharge cycles that spoiled a battery leads to a short lifetime of this and the efficiency is reduced by up to 40% at the end of the year of use. As well as the ratio of electrical energy returned by the system EL-FC over its lifetime to the electrical equivalent energy required to build this system. Furthermore the components of the battery are less environment friendly with high amount of pollutants. The lifetime estimation of our system is about 20 years as many referees have reported [39–42].

$$f_{PV} = \frac{E_{e,PVnm}}{E_{e,PV30m}} \quad (2)$$

Our system contains in total ninety PV modules and considering that one PV module area is 0.868 m², the total area of the solar PV array is 78.12 m², which perfectly fits the standard dimensions of the roof of the house. This final value agrees well with those of solar PV array areas found in other studies for similar applications, whose calculation approaches were: 65.2 m² for a PV system integrated into a one-family house at Zollbrück, Switzerland [43] and 65 m² as the optimal area for direct coupling between solar PV array and a proton exchange membrane water electrolyzer [26].

3.2 AEMWE Electrolyzer

In this work we have used for the coupling, Fig. 5, the current-potential curves experimentally obtained in our lab with a self-prepared membrane electrode assembly (MEA). It is based on two electrodes, anode and cathode, made of metallic Ni-Fe sputtered by magnetron sputtering technique [26,44–46] on Carbon Gas Diffusion Layers (GDL), and a Fumapem FAA-3-50 membrane [4] and located in the middle of both electrodes [47]. The electrolysis unit also includes a corrosion resistant 5 cm² anode and cathode nickel flow fields. For this work a polarization curve of this experimental electrolyzer is used for the coupling, Fig. 5. The experimentation to obtain the sweep voltammetry was carried out in a potassium hydroxide solution (1 M) at 40 ºC temperature.

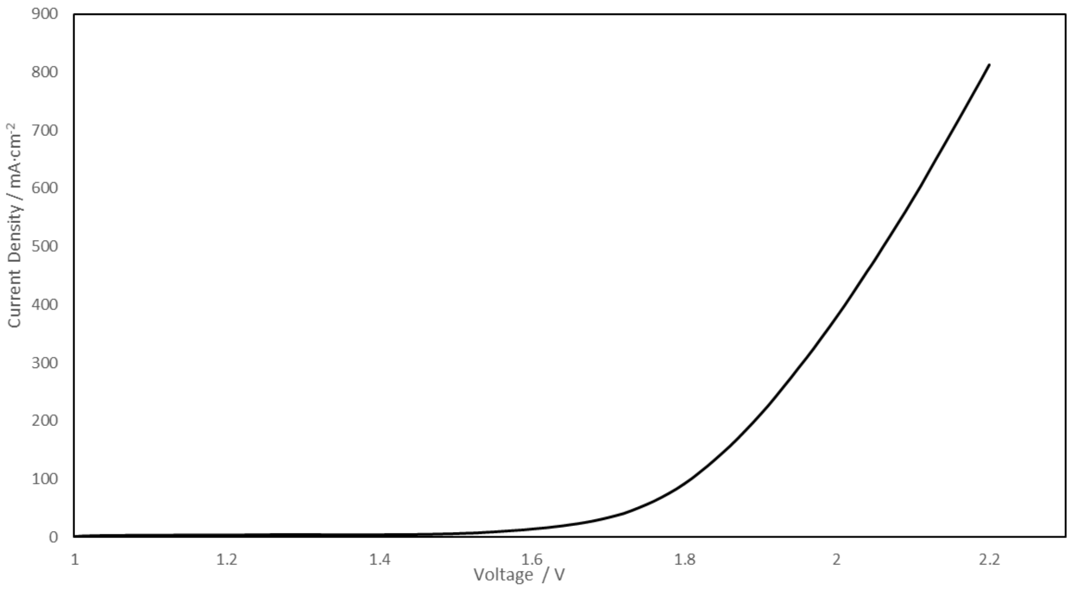

According to previous studies [18,26], the most efficient coupling of the PV module with the experimental electrolyzer occurs at the maximum power point of the PV module at the highest radiation level, 1000 W/m². However, the maximum power point of the experimental electrolyzer is much lower than that of the PV module. In terms of current, the maximum current of the PV module is close to the maximum value of the experimental electrolyzer. However, it is not possible in terms of voltage since electric potential of the electrolyzer is much lower. For this reason, the number of cells in series in the electrolyzer must be modified until reaching the maximum power point of the PV module, whose coupling is showed in Fig. 6.

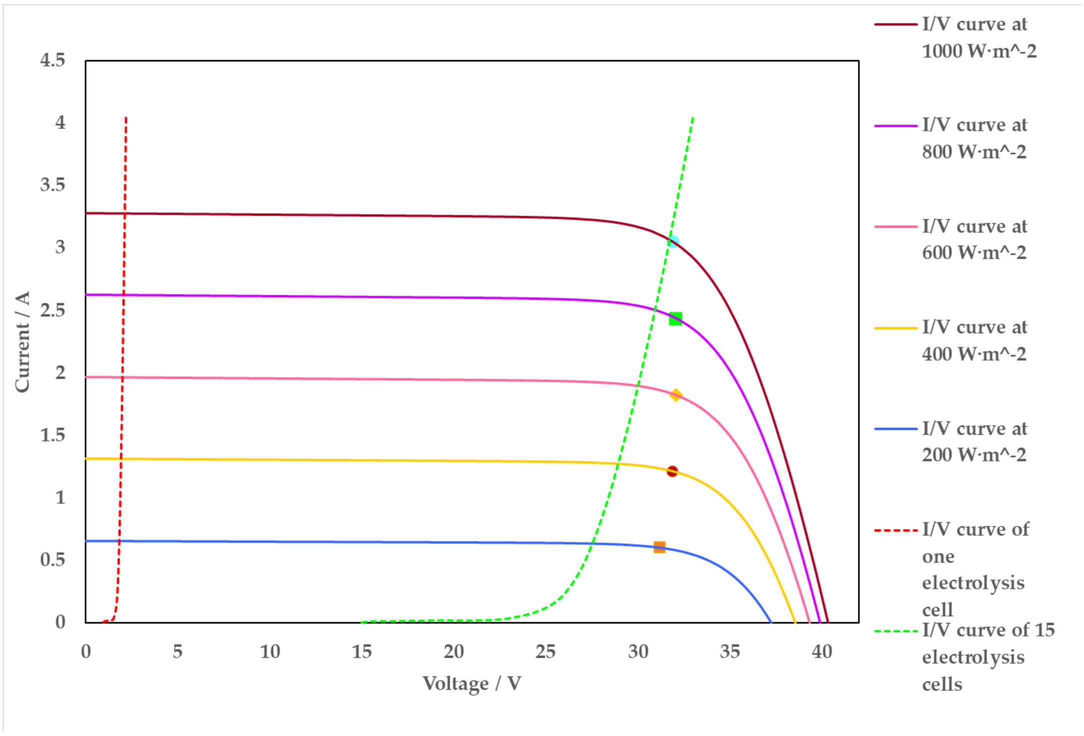

As can be observed from Fig. 6, fifteen AEMWE cells are required per PV module for reaching the maximum power point of the PV module. It means that a high number of cells will be required for the ninety PV modules. This is due to the low geometric area of the electrodes (5 cm²) of the experimental lab scale electrolyzer used. Hence, considering that the electrode area of a commercial AEM electrolyzer is typically between 50 cm²-200 cm², selecting the area of the electrolyzer is a good approach for obtaining a system of big-scale and reduces the number of electrolyzer cells into the stack. According to the polarization curve, Fig. 5, the I-V curve for an electrolyzer with an area of 50 cm² is obtained through it (Fig. S3). Hence, considering that the maximum current point of the electrolyzer (I_{MPP}) is 40 A, the last PV module is not a good approach for this new coupling. For this reason, a new PV module with more current than the last one must be chosen. The selected PV model is Solartec SSW72 08 108Wp module, with a maximum current per module of 8 A. For this reason, a PV string with five PV modules in parallel is required to reach 40 A of current. It was not necessary with the 5 cm² electrolyzer since the maximum current point was 4 A as the PV module point, the coupling in terms of current was fixed. I-V curve of the selected module is shown in the supporting information, Fig. S4.

Following the same procedure explained for the electrolyzer of 5 cm² (Figure 3), the number of PV string required by the electrolyzer of 50 cm² was found to be five. This optimization of the number of PV strings in series is shown in the supporting information, Fig. S5. Applying the sizing factor obtained in section 3.1 by Eq. (2), fifteen PV strings are required by the system EL-FC, and seventy-five PV modules are contained in the solar PV array for the coupling with EL-FC system. The area of solar PV array is 65.325 m² considering the photovoltaic module area is 0.871 m², which are close to those reported in the available literature [26,43].

As can be observed from the coupling shown in Fig. 7, six electrolyzer cells are required per PV string for reaching the maximum power point. According to this, the total number of electrolyzer cells is really lower than before, thirty electrolyzer cells required by the solar PV array.

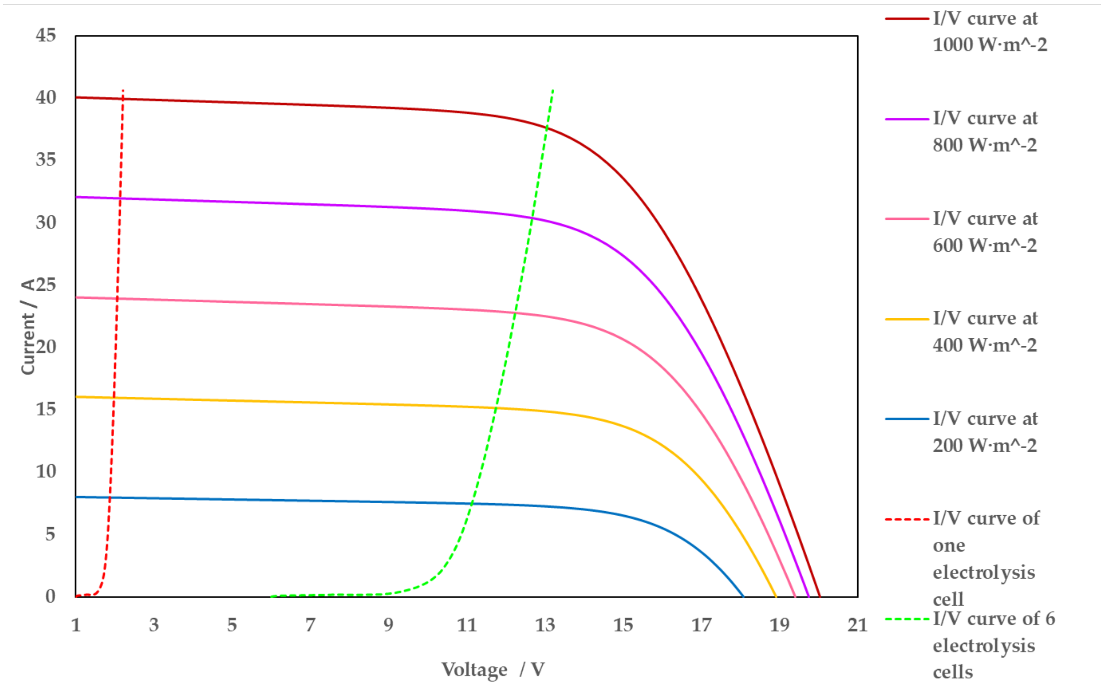

Figure 7. Coupling Solartec SSW72 08 108Wp PV module -50 cm^2 AEMWE developed in our lab

3.3 Fuel Cell

In this section, the aim is the selection of an appropriate fuel cell. On the daily demand per hour of the one-family house (see Fig. 1), the peak maximum of electrical power is achieved at 8 pm, 1.015 kW. The selected fuel cell must be available for supplying this power demand when the solar energy is null. Considering this, the maximum power per hour that the fuel cell must supply is 1.218 kW according to a 20% of oversizing. A possible commercially available option among different manufacturers is the model Fcgen-1020ACS, which is a proton exchange membrane (PEMFC) that can be scaled up to meet power requirements from 450 W to 3 kW. The physical characteristics per stack of fifty-six fuel cells is 363x103x351 mm, being the fuel flow rate per fuel cell 0.5 standard liter per minute (slpm) and the rated power 41.1W/cell. It is an air-cooled fuel cell stack with open-cathode and a self-humidifying MEA which allows to eliminate the humidifier, coolant pump and radiator. Therefore, to cover the power of 1.218 kW, thirty fuel cells are necessary in the FC stack. For more information of the fuel cell, see Fig. S6 in the supporting information.

An estimation of the hydrogen consumption is taken into account since the Ballard manufacturer provides the consumption of hydrogen, 0.5 L/min per cell. In terms of mass, 0.059 kg/ day per cell. Besides, this hydrogen consumption is for a production of 30 kWh per day. As in our system, the maximum electrical demand per day is 7.635 kWh, the fuel cell consumes 0.45 kg for obtaining this energy. For this reason, considering the design basis of four consecutive days without solar energy, the amount of hydrogen that must be stored in the tank is 1.8 kg.

3.4 Hydrogen tank

Different methods have been reported for hydrogen storage as hydrogen hydrates, which have been compared in bibliography with existing hydrogen storage technologies [47,48]. This type of storage is useful when a large distance transport is required [49,50]. However, for low scale application and for single entry production-consumption, the compressed hydrogen storage (CGH_2) is the best choice. In this study a typical mathematic method for design of pressurized tanks has been used [51]. The main design basis are the conditions and amount of hydrogen to be stored (1.8 kg, as already mentioned). A commercial AEMWE, such as the ones commercialized, achieved the maximum hydrogen pressure conditions of 35 bars [52]. Hence, for the current study, the pressure and temperature conditions are fixed in 30 bars and 298 K. Due to this outlet pressure, a compressor is not required for this residential application. The tank volume is calculated by the equation of Mench [19,51] defined as follows:

$$\frac{P}{n^3}\cdot V^3+\left(-\frac{P\cdot b}{n^2}-\frac{Ru\cdot T}{n^2}\right)\cdot V^2+\frac{a}{n}\cdot V-a\cdot b=0 \quad (3)$$

where P is the pressure (3x10^6 Pa), V is the tank volume (m^3), n is the number of moles (900), Ru is universal gas constant (8.314 J/mol K), T is the temperature (298 K), and a and b are constant calculated by equations (4) and (5), respectively.

$$a=\frac{27}{64}\cdot\frac{R_u^2\cdot T_c^2}{Pc} \quad (4)$$

$$b=\frac{Ru}{8}\cdot\frac{Tc}{Pc} \quad (5)$$

where T_c is the critical temperature and P_c is the critical pressure of the hydrogen gas. Hydrogen initial conditions are collected in Table S2. All this allows to calculate the tank volume achieving a theoretical value of 0.758 m^3. Considering an oversizing of 20%, a final volume of 0.91 m^3 is obtained for the hydrogen tank. Concerning the recipient material, carbon steel is the preferred one for indoor pressure equipment according to the ASME BPVC Section VIII code [53]. Future developments of new composite materials would increase the tensile strength above that of steel, although most of reports use a wide range of steel types, e.g. stainless steel [54]. Then, the specific dimensions of the hydrogen tank are calculated using the Mijalev monogram (see Fig. S7 in the SI) [55] which shows two axes, reduced pressure (MPa) and tank volume (m^3). Reduced pressure is estimated with Eq. (6):

$$Pred=\frac{Pcal}{10\cdot[\sigma]\cdot C} \quad (6)$$

where P_{red} is the reduced pressure (MPa), P_{cal} is the calculation pressure (3.6 MPa), $[\sigma]$ is the permissible tension of carbon steel (107.1 MPa) and C is the overthickness by corrosion (0.002 m). These parameters are according to carbon steel material [52].

Once the tank volume (0.91 m^3) and reduced pressure (1.6807 MPa) are calculated, the Mijalev monogram is used to know the optimal diameter, 0.7 m. As the tank is cylindrical, the height is calculated with the diameter and volume. The optimal dimensions are 2.4 m x 0.7 m.

As it is an indoor pressure tank, the shell is indispensable for the safety of the system [51]. The thickness of the shell is calculated according to the Eq. (7):

$$S_{cal}=max\left\{\frac{Pdesign\cdot D}{2\cdot\emptyset\cdot[\sigma]-Pdesign};\frac{P_{test}\cdot D}{2\cdot\emptyset\cdot[\sigma]test-Ptest}\right\} \quad (7)$$

where S_{cal} is the shell thickness (m), P_{design} is the indoor pressure tank ($3*10^6$ Pa), D is the diameter (0.7 m), ϕ is the welding factor (1), $[\sigma]$ is the permissible tension of carbon steel ($107.1x10^6$ Pa), P_{test} is the test pressure ($4.5x10^6$ Pa), and $[\sigma]_{test}$ is the test permissible tension ($97.364x10^6$ Pa) [56–58].

To sum up, the shell thickness obtained is 0.0166 m. Besides, an overthickness by corrosion of 0.002 m is taken into account following the ASME code [53]. Then, the total thickness of the shell is 0.0186 m. The final dimensions are graphically shown in the supporting information, Fig. S8. This design method considers the design criteria that the amount of material is minimum. For this reason, an optimization of material is automatically made.

4. Economic evaluation estimation.

In this section, a preliminary economic analysis of the proposed system is performed. Followed by the economic comparation with the concentional system with battery. Some parameters have been considered like Levelized Cost of Energy (LCOE) which is taken for evaluating the cost of the system, the *LCOE* value can be calculated through the Nizetic et al. equation [59,60]:

$$LCOE = \frac{ICxCRF + OM}{EO} \quad (8)$$

where *IC* is installation cost, *OM* is operation and maintenance cost, *CRF* is capital recovery factor and *EO* is average annual overall energy output from the system. The *CRF* factor is calculated according the next equation:

$$CRF = \frac{(1+p)^n \cdot p}{(1+p)^n - 1} \quad (9)$$

where p is the interest rate and n is the amortization period. In this case, the interest rate is 10% and twenty years of amortization period.

Furthermore, two economic parameters have been calculated for clarifying the financial part. On the one hand, the Net Present Value (NPV) which is an economic tool used to equate the total cost of a project over a specified time period to the total cost today, taking into account the time value of money. On the other hand, the Internal Rate of Return (IRR) which is a financial parameter to estimate the profibility of potential investments [27,61].

$$NPV = \sum_{0}^{n} \frac{C}{(1+i)^n} \quad (10)$$

The equipment investment is shown in the Table 2. The price of the photovoltaic panel, the electrolyzer, the fuel cell and the battery are the real prices that the corresponding companies are selling it. However, the cost of the hydrogen tank was calculated in order to the amount of carbon steel required, following the next equation:

$$m = \rho \cdot S \cdot \left(\frac{4 \cdot V}{D} + 1.04 \cdot D^2\right) \quad (11)$$

Table 2. Equipment investment for both systems: the electrolyzer-fuel cell system without battery and the conventional system (photovoltaic panel with battery).

SYSTEM	EQUIPMENT	Cost (€)	TOTAL (€)
EL-FC	Photovoltaic Panel	3,052	**12,827**
	Electrolyzer	5,493	
	Fuel Cell	2,436	
	Hydrogen Tank	1,846	
BATTERY	Photovoltaic Panel	3,562	**10,835**
	Battery	7,273	

Once known the equipment investment, the rest of investments are calculated by the Vian Method (see Table S3 in the S.I), following it the total investment is 15,803 € and 13,348 € for EL-FC system and conventional system, respectively. The datasheet of the battery indicate that the efficiency of 90% is only keeping for a year of use. According to this design, a new battery has to be bought every year because the design was carried out with this efficiency. The rest of equipments have roughly a life of 20 years of use as many researchers have supported[62,63]. For this reason, the investment period is 20 years.

The aim of the economic evaluation is obtained the value of above mentioned parameters for comparing the systems (NPV, IRR, CRF, LCOE). For this, a serie of parameters is required like fixed capital investment, working capital investment (10% of the fixed capital investment), invested funds, benefits, amortization and cash flow (see **Figure S4** in the S.I).

According to the economic results, LCOE value of our system is higher than the conventional system due to the novelty of our system which involves an anion exhange membrane water electrolyzer little developed so far, corresponding to a high cost. Although the values of LCOE are coming up between both and similar to another reports [64,65]. Currently, the conventional system presented a more sympathetic economic part since the NPV and IRR is higher, 2,164 and 12,31%, respectively. The main barrier for El-FC system is their high initial investment cost and the reliability of novel energy technologies.

Table 3. Results of the economic evaluation for both systems.

SYSTEM	NPV (€)	IRR (%)	LCOE (€/kWh)
EL-FC	660	10.61	0.541
BATTERY	2,164	12.31	0.534

AÑADIR GRÁFICA COMPARANDO LCOE CON OTROS PAPERS. (JUEVES)

5. Conclusions

The obtained results demonstrate that the introduction of hydrogen and photovoltaic system into a domestic application is a viable option to supply energy without any connection to the grid. For isolated locations from the electricity grid this method of coupling is a good approach to produce energy.

The design takes place in Spain, but the procedure developed on this work can be generally use elsewhere since it implies the use of a commercial PV software and available general information.

The present study is based on a novel and simple procedure to design a photovoltaic-hydrogen system, but the obtained sizing results of the different components are in good agreement with previous studies which typically used more complex models or experimental procedures which supports the information reported here.

An initial solar PV array is calculated by using the commercial software PV-SYST 7.0, which considers the energy storage within a battery. However, in next steps the battery is replaced by the electrolyzer-fuel cell system because the battery has a short lifetime and charge/discharge cycles. Furthermore, the battery components are less friendly with the environment. From this way, the study gets the most sustainable way of produce energy in an isolated location. These results demonstrate that is possible to use hydrogen for self-sufficient energy system for low scale domestic application as an alternative method to conventionally used batteries.

This study leads to an increase in the final area of the solar PV array to a final value of 65.325 m^2, which is feasible within the standard dimensions of the roof of a house and agrees well with previous results published in the literature. The optimal final dimensions of the hydrogen tank were found to be 2.4 x 0.7 m at 30 bars as storage pressure, being the selected material carbon steel. These dimensions are close to the dimensions of the diesel tank that nowadays being at home. As well as the final number of cells in the electrolyzer has been calculated according to the commercial AEMWE units available in the market. Also, a PEM fuel cell is chosen in order to achieve the maximum power required in the application. All the equipment's can be laid down in anyone-family house.

Nomenclature

BA Battery
E_{EL} Consumed energy by the electrolyzer per kg of hydrogen, 45.29 kWh/kgH_2
I Current, A
η_{BA} Efficiency of battery, 0.9
η_{FC} Efficiency of fuel-cell, 0.65
D Electrical demand, Wh/day or kWh/day
S_{EL} Electrolyzer area
EL Electrolysis cell
E Energy, kWh
E_{BAe} Energy of the extra battery, kWh/day
E_e Excess energy, kWh/day
BA_e Extra battery
FC Fuel-Cell
HT Hydrogen tank
E_i Input energy, kWh/day
$E_{i,EL}$ Input energy of electrolyzer, kWh/day
N_{EL} Number of EL cells in series
N_{PV} Number of PV modules in series
PV_{1m} One photovoltaic module
$S_{o,EL}$ Optimal area of electrolyzer
$N_{PV,OP}$ Optimal number of PV modules in series
E_o Output energy, kWh/day
$E_{o,BA}$ Output energy of battery, kWh
$E_{o,FC}$ Output energy of fuel-cell, kWh/day
$E_{o,PVnm}$ Output energy of *n* photovoltaic module, kWh/day; *n*: number of photovoltaic modules.
$P_{o,FC}$ Output power of fuel-cell, kW
OT Oxygen tank
S_{PVp} Photovoltaic array area
S_{PVm} Photovoltaic module area
P Power, kW
I_{MPP} PV Current at the maximum power point (MPP), A
V_{MPP} PV Voltage at the maximum power point (MPP), V
f_{EL} Sizing factor of electrolyzer
f_{PV} Sizing factor of photovoltaic panel
PV_P Solar PV array
G Solar radiation, W/m^2
S_{SEL} Stack electrolyzer area
SEL Stack of electrolysis cells
t time, hour or day
V Voltage, V

Supplementary Materials: The following are available online at www.mdpi.com/xxx/s1, Figure S1: P&ID. Figure S2: I-V characteristic curves of Solartec_SST72_110_24_106W module. Figure S3: I-V curve of the experimental AEMWE of 50 cm^2. Figure S4: I-V characteristic curves of Solartec_SSW72_08_108Wp module. Figure S5: January supplied electrical demand by a) three PV string for the 1st b) three PV string for the first week c) four PV string for the first week d) four PV string for the full month e) five PV string for the full month. Figure S6: Datasheet of Fcgen-1020ACS fuel-cell. Figure S7: Mijalev monogram. Figure S8: Hydrogen tank with dimensions.

Table S1: Output photovoltaic panel energy and electrolyzer energy. Table S2: Hydrogen initial conditions.

Acknowledgments: Authors thank the 'Fundación DOMINGO MARTINEZ' for financial support.

Conflicts of Interest: The authors declare no conflict of interest.

References

1. Amores, E.; Rodríguez, J.; Carreras, C. Influence of operation parameters in the modeling of alkaline water electrolyzers for hydrogen production. *Int. J. Hydrogen Energy* **2014**, *39*, 13063–13078, doi:10.1016/j.ijhydene.2014.07.001.
2. Siegel, A.; Schott, T. Optimization of photovoltaic hydrogen production. *Int. J. Hydrogen Energy* **1988**, *13*, 659–675, doi:10.1016/0360-3199(88)90076-6.
3. López-Fernández, E.; Gil-Rostra, J.; Espinós, J.P.; González-Elipe, A.R.; Yubero, F.; de Lucas-Consuegra, A. CuxCo3-xO4 ultra-thin film as efficient anodic catalysts for anion exchange membrane water electrolysers. *J. Power Sources* **2019**, *415*, 136–144, doi:10.1016/j.jpowsour.2019.01.056.
4. López-Fernández, E.; Gil-Rostra, J.; Espinós, J.P.; González-Elipe, A.R.; De Lucas Consuegra, A.; Yubero, F. Chemistry and Electrocatalytic Activity of Nanostructured Nickel Electrodes for Water Electrolysis. *ACS Catal.* **2020**, *10*, 6159–6170, doi:10.1021/acscatal.0c00856.
5. Caravaca, A.; Sapountzi, F.M.; De Lucas-Consuegra, A.; Molina-Mora, C.; Dorado, F.; Valverde, J.L. Electrochemical reforming of ethanol-water solutions for pure H 2 production in a PEM electrolysis cell. *Int. J. Hydrogen Energy* **2012**, *37*, 9504–9513, doi:10.1016/j.ijhydene.2012.03.062.
6. González-Cobos, J.; Valverde, J.L.; de Lucas-Consuegra, A. Electrochemical vs. chemical promotion in the H2 production catalytic reactions. *Int. J. Hydrogen Energy* **2017**, *42*, 13712–13723, doi:10.1016/j.ijhydene.2017.03.085.
7. Kelly, N.A. *Hydrogen production by water electrolysis*; 2014; ISBN 9780857097736.
8. Maeda, T.; Ito, H.; Hasegawa, Y.; Zhou, Z.; Ishida, M. Study on control method of the stand-alone direct-coupling photovoltaic - Water electrolyzer. *Int. J. Hydrogen Energy* **2012**, *37*, 4819–4828, doi:10.1016/j.ijhydene.2011.12.013.
9. Khalilnejad, A.; Riahy, G.H. A hybrid wind-PV system performance investigation for the purpose of maximum hydrogen production and storage using advanced alkaline electrolyzer. *Energy Convers. Manag.* **2014**, *80*, 398–406, doi:10.1016/j.enconman.2014.01.040.
10. Chaparro, A.M.; Soler, J.; Escudero, M.J.; De Ceballos, E.M.L.; Wittstadt, U.; Daza, L. Data results and operational experience with a solar hydrogen system. *J. Power Sources* **2005**, *144*, 165–169, doi:10.1016/j.jpowsour.2004.12.044.
11. Erdinc, O.; Uzunoglu, M. A new perspective in optimum sizing of hybrid renewable energy systems: Consideration of component performance degradation issue. *Int. J. Hydrogen Energy* **2012**, *37*, 10479–10488, doi:10.1016/j.ijhydene.2012.04.071.
12. Sánchez, M.; Amores, E.; Rodríguez, L.; Clemente-Jul, C. Semi-empirical model and experimental validation for the performance evaluation of a 15 kW alkaline water electrolyzer. *Int. J. Hydrogen Energy* **2018**, *43*, 20332–20345, doi:10.1016/j.ijhydene.2018.09.029.
13. Teichmann, D.; Arlt, W.; Wasserscheid, P. Liquid Organic Hydrogen Carriers as an efficient vector for the

transport and storage of renewable energy. *Int. J. Hydrogen Energy* **2012**, *37*, 18118–18132, doi:10.1016/j.ijhydene.2012.08.066.
14. Reuß, M.; Grube, T.; Robinius, M.; Preuster, P.; Wasserscheid, P.; Stolten, D. Seasonal storage and alternative carriers: A flexible hydrogen supply chain model. *Appl. Energy* **2017**, *200*, 290–302, doi:10.1016/j.apenergy.2017.05.050.
15. Niermann, M.; Timmerberg, S.; Drünert, S.; Kaltschmitt, M. Liquid Organic Hydrogen Carriers and alternatives for international transport of renewable hydrogen. *Renew. Sustain. Energy Rev.* **2021**, *135*, 110171, doi:10.1016/j.rser.2020.110171.
16. García-Valverde, R.; Espinosa, N.; Urbina, A. Optimized method for photovoltaic-water electrolyser direct coupling. *Int. J. Hydrogen Energy* **2011**, *36*, 10574–10586, doi:10.1016/j.ijhydene.2011.05.179.
17. Ozden, E.; Tari, I. Energy-exergy and economic analyses of a hybrid solar-hydrogen renewable energy system in Ankara, Turkey. *Appl. Therm. Eng.* **2016**, *99*, 169–178, doi:10.1016/j.applthermaleng.2016.01.042.
18. Gutiérrez-Martín, F.; Calcerrada, A.B.; de Lucas-Consuegra, A.; Dorado, F. Hydrogen storage for off-grid power supply based on solar PV and electrochemical reforming of ethanol-water solutions. *Renew. Energy* **2020**, *147*, 639–649, doi:10.1016/j.renene.2019.09.034.
19. Budak, Y.; Devrim, Y. Comparative study of PV/PEM fuel cell hybrid energy system based on methanol and water electrolysis. *Energy Convers. Manag.* **2019**, *179*, 46–57, doi:10.1016/j.enconman.2018.10.053.
20. Index @ Www.Pvsyst.Com.
21. Mermoud, A.; Lejeune, T. Performance Assessment of a Simulation Model for Pv Modules of Any Available Technology. *25th Eur. PV Sol. Energy Conf.* **2010**, 6–10.
22. ECONOMIC OPTIMIZATION OF PV SYSTEMS WITH STORAGE André Mermoud, Adrien Villoz, Bruno Wittmer, Hizir Apaydin PVsyst SA Route de la Maison-Carrée 30, CH 1242 Satigny, Switzerland.
23. Zablocki, A. Energy storage: Fact sheet (2019). *Eesi* **2019**, *2040*, 1–8.
24. Gibson, T.L.; Kelly, N.A. Optimization of solar powered hydrogen production using photovoltaic electrolysis devices. *Int. J. Hydrogen Energy* **2008**, *33*, 5931–5940, doi:10.1016/j.ijhydene.2008.05.106.
25. Behzadi, M.S.; Niasati, M. Comparative performance analysis of a hybrid PV/FC/battery stand-alone system using different power management strategies and sizing approaches. *Int. J. Hydrogen Energy* **2015**, *40*, 538–548, doi:10.1016/j.ijhydene.2014.10.097.
26. Clarke, R.E.; Giddey, S.; Ciacchi, F.T.; Badwal, S.P.S.; Paul, B.; Andrews, J. Direct coupling of an electrolyser to a solar PV system for generating hydrogen. *Int. J. Hydrogen Energy* **2009**, *34*, 2531–2542, doi:10.1016/j.ijhydene.2009.01.053.
27. Al-Khori, K.; Bicer, Y.; Koç, M. Comparative techno-economic assessment of integrated PV-SOFC and PV-Battery hybrid system for natural gas processing plants. *Energy* **2021**, *222*, 119923, doi:10.1016/j.energy.2021.119923.
28. Amores, E.; Sánchez, M.; Rojas, N.; Sánchez-Molina, M. Renewable hydrogen production by water electrolysis. In *Sustainable Fuel Technologies Handbook*; Elsevier, 2021; pp. 271–313.
29. Zhang, X.; Ni, M.; Wang, J.; Yang, L.; Mao, X.; Su, S.; Yang, Z.; Chen, J. Configuration design and parametric optimum selection of a self-supporting PEMFC. *Energy Convers. Manag.* **2020**, *225*, doi:10.1016/j.enconman.2020.113391.
30. Fan, L.; Tu, Z.; Chan, S.H. Recent development of hydrogen and fuel cell technologies: A review. *Energy Reports* **2021**, doi:10.1016/j.egyr.2021.08.003.
31. Wishart, J.; Dong, Z.; Secanell, M. Optimization of a PEM fuel cell system based on empirical data and a generalized electrochemical semi-empirical model. *J. Power Sources* **2006**, *161*, 1041–1055,

doi:10.1016/j.jpowsour.2006.05.056.
32. Cheng, S.; Xu, L.; Wu, K.; Fang, C.; Hu, J.; Li, J.; Ouyang, M. Optimal warm-up control strategy of the PEMFC system on a city bus aimed at improving efficiency. *Int. J. Hydrogen Energy* **2017**, *42*, 11632–11643, doi:10.1016/j.ijhydene.2017.02.203.
33. Authayanun, S.; Wiyaratn, W.; Assabumrungrat, S.; Arpornwichanop, A. Theoretical analysis of a glycerol reforming and high-temperature PEMFC integrated system: Hydrogen production and system efficiency. *Fuel* **2013**, *105*, 345–352, doi:10.1016/j.fuel.2012.07.036.
34. Witkowski, A.; Rusin, A.; Majkut, M.; Stolecka, K. Comprehensive analysis of hydrogen compression and pipeline transportation from thermodynamics and safety aspects. *Energy* **2017**, *141*, 2508–2518, doi:10.1016/j.energy.2017.05.141.
35. Møller, K.T.; Jensen, T.R.; Akiba, E.; Li, H. wen Hydrogen - A sustainable energy carrier. *Prog. Nat. Sci. Mater. Int.* **2017**, *27*, 34–40, doi:10.1016/j.pnsc.2016.12.014.
36. Castañeda, M.; Cano, A.; Jurado, F.; Sánchez, H.; Fernández, L.M. Sizing optimization, dynamic modeling and energy management strategies of a stand-alone PV/hydrogen/battery-based hybrid system. *Int. J. Hydrogen Energy* **2013**, *38*, 3830–3845, doi:10.1016/j.ijhydene.2013.01.080.
37. de Andrade, G.A.; Mendes, P.R.C.; García-Clúa, J.G.; Normey-Rico, J.E. Control of a grid assisted PV-H2 production system: A comparative study between optimal control and hybrid MPC. *J. Process Control* **2020**, *92*, 220–233, doi:10.1016/j.jprocont.2020.06.008.
38. Amores, E.; Rodríguez, J.; Oviedo, J.; De Lucas-Consuegra, A. Development of an operation strategy for hydrogen production using solar PV energy based on fluid dynamic aspects. *Open Eng.* **2017**, *7*, 141–152, doi:10.1515/eng-2017-0020.
39. Pellow, M.A.; Emmott, C.J.M.; Barnhart, C.J.; Benson, S.M. Hydrogen or batteries for grid storage? A net energy analysis. *Energy Environ. Sci.* **2015**, *8*, 1938–1952, doi:10.1039/c4ee04041d.
40. Motealleh, B.; Liu, Z.; Masel, R.I.; Sculley, J.P.; Richard Ni, Z.; Meroueh, L. Next-generation anion exchange membrane water electrolyzers operating for commercially relevant lifetimes. *Int. J. Hydrogen Energy* **2021**, *46*, 3379–3386, doi:10.1016/j.ijhydene.2020.10.244.
41. Liu, S.; Wang, J.; Liu, H.; Liu, Q.; Tang, J.; Li, Z. Battery degradation model and multiple-indicators based lifetime estimator for energy storage system design and operation: Experimental analyses of cycling-induced aging. *Electrochim. Acta* **2021**, *384*, 138294, doi:10.1016/j.electacta.2021.138294.
42. Harrison, K. 2 nd International Workshop Durability and Degradation Issues in PEM Electrolysis Cells and its Components Life-Time Prediction of PEM Water Electrolysis Stacks Coupled With RES Transportation. **2016**.
43. Hollmuller, P.; Joubert, J.M.; Lachal, B.; Yvon, K. Evaluation of a 5 kWp photovoltaic hydrogen production and storage installation for a residential home in Switzerland. *Int. J. Hydrogen Energy* **2000**, *25*, 97–109, doi:10.1016/S0360-3199(99)00015-4.
44. Li, H.; Gao, Y.-J.; Yuan, S.-H.; Wuu, D.-S.; Wu, W.-Y.; Zhang, S. Improvement in the Figure of Merit of ITO-Metal-ITO Sandwiched Films on Poly Substrate by High-Power Impulse Magnetron Sputtering. *Coatings* **2021**, *11*, 144, doi:10.3390/coatings11020144.
45. Ababneh, A.; Dagamseh, A.M.K.; Albataineh, Z.; Tantawi, M.; Al-Bataineh, Q.M.; Telfah, M.; Zengerle, T.; Seidel, H. Optical and structural properties of aluminium nitride thin-films synthesized by DC-magnetron sputtering technique at different sputtering pressures. *Microsyst. Technol.* **2021**, *4*, doi:10.1007/s00542-020-05081-4.
46. Cho, S. Properties of Eu - doped - YVO 4 thin films grown on glass substrates by radio - frequency magnetron sputtering. *Appl. Phys. A* **2021**, 1–6, doi:10.1007/s00339-021-04308-z.

47. Liu, Z.; Sajjad, S.D.; Gao, Y.; Yang, H.; Kaczur, J.J.; Masel, R.I. The effect of membrane on an alkaline water electrolyzer. *Int. J. Hydrogen Energy* **2017**, *42*, 29661–29665, doi:10.1016/j.ijhydene.2017.10.050.
48. Di Profio, P.; Arca, S.; Rossi, F.; Filipponi, M. Comparison of hydrogen hydrates with existing hydrogen storage technologies: Energetic and economic evaluations. *Int. J. Hydrogen Energy* **2009**, *34*, 9173–9180, doi:10.1016/j.ijhydene.2009.09.056.
49. Ozaki, M.; Tomura, S.; Ohmura, R.; Mori, Y.H. Comparative study of large-scale hydrogen storage technologies: Is hydrate-based storage at advantage over existing technologies? *Int. J. Hydrogen Energy* **2014**, *39*, 3327–3341, doi:10.1016/j.ijhydene.2013.12.080.
50. Niermann, M.; Timmerberg, S.; Drünert, S.; Kaltschmitt, M. Liquid Organic Hydrogen Carriers and alternatives for international transport of renewable hydrogen. *Renew. Sustain. Energy Rev.* **2021**, *135*, 110171, doi:10.1016/j.rser.2020.110171.
51. 9780470209769 @ onlinelibrary.wiley.com.
52. index @ www.enapter.com.
53. ASME BPVC, Section VIII, DIV 1. **2015**.
54. Züttel, A. Hydrogen storage methods. *Naturwissenschaften* **2004**, *91*, 157–172, doi:10.1007/s00114-004-0516-x.
55. https://www.bing.com/images/search?view=detailV2&id=64EC46C8A1A5857C046AA634888B7E93E3EA370C&thid=OIP.orQg-hMQc_l5qgqKkZezOwHaGH&mediaurl=http%3A6F6Fsumozade.com6Fsg90-9g-micro-servo-motor-1902-62-B.jpg&exph=744&expw=900&q=motor+servo&selectedindex=0&ajax, 6; 19-08-2019 Search @ Www.Bing.Com. *Hosp. Univ. la Ribera* 2014, www.bing.com.
56. 0884156478 @ www.amazon.es.
57. Manual_de_Recipientes_a_Presion_Megyesy_1_ @ www.academia.edu.
58. 978-0-08-049255-1 @ www.elsevier.com.
59. Nižetić, S.; Tolj, I.; Papadopoulos, A.M. Hybrid energy fuel cell based system for household applications in a Mediterranean climate. *Energy Convers. Manag.* **2015**, *105*, 1037–1045, doi:10.1016/j.enconman.2015.08.063.
60. Nižetić, S.; Duić, N.; Papadopulos, A.M.; Tina, G.M.; Grubišić-Čabo, F. Energy efficiency evaluation of a hybrid energy system for building applications in a Mediterranean climate and its feasibility aspect. *Energy* **2015**, *90*, 1171–1179, doi:10.1016/j.energy.2015.06.053.
61. Domingos, R.M.A.; Pereira, F.O.R. Comparative cost-benefit analysis of the energy efficiency measures and photovoltaic generation in houses of social interest in Brazil. *Energy Build.* **2021**, *243*, 111013, doi:10.1016/j.enbuild.2021.111013.
62. Budak, Y.; Devrim, Y. Investigation of micro-combined heat and power application of PEM fuel cell systems. *Energy Convers. Manag.* **2018**, *160*, 486–494, doi:10.1016/j.enconman.2018.01.077.
63. Uhm, S.; Jeon, H.; Kim, T.J.; Lee, J. Clean hydrogen production from methanol-water solutions via power-saved electrolytic reforming process. *J. Power Sources* **2012**, *198*, 218–222, doi:10.1016/j.jpowsour.2011.09.083.
64. Gökçek, M.; Kale, C. Optimal design of a Hydrogen Refuelling Station (HRFS) powered by Hybrid Power System. *Energy Convers. Manag.* **2018**, *161*, 215–224, doi:10.1016/j.enconman.2018.02.007.
65. Isa, N.M.; Das, H.S.; Tan, C.W.; Yatim, A.H.M.; Lau, K.Y. A techno-economic assessment of a combined heat and power photovoltaic/fuel cell/battery energy system in Malaysia hospital. *Energy* **2016**, *112*, 75–90, doi:10.1016/j.energy.2016.06.056.